High-Sensitivity Micro-LED-Based Fingerprint Recognition System Using Charge Integrators and Differential Sensing Method

Su-Hyeong Kim, Won-Been Jeong*, Hyun-Gi Kim**, Jung-Hyun Kim**, Hoon-Ju Chung***, and Seung-Woo Lee**

***Dept. of Information Display, Kyung Hee University, Seoul, Korea**
****MicroLED Convergence Research Center, Korea Photonics Technology Institute, Gwangju, Korea**
*****School of Electronic Engineering, Kumoh National Institute of Technology, Gumi, Korea**

Abstract

This paper proposes a high-sensitivity micro-LED-based fingerprint recognition system without any additional sensors. It is proposed to adopt charge integrators for readout circuits and differential sensing method to eliminate electronic noise for high-sensitivity. Although photocurrent difference between ridge and valley is as small as 4.56 nA, the proposed system successfully produces a 1.38 V readout voltage difference in 300 μs. This demonstrates that the proposed system recognizes various fingerprint patterns across the entire display screen with high-sensitivity.

Author Keywords

Micro-LED; Fingerprint Recognition; High-Sensitivity; Charge Integrator; Differential Sensing Method.

1. Introduction

With the advancement of mobile displays, users can now perform various functions such as financial transactions and identity verification through their smartphones. Consequently, the amount of personal data stored on smartphones has rapidly increased, and the importance of security systems to protect personal data has grown significantly. Among the various security methods, fingerprint recognition is the most widely used due to its convenient accessibility and high security.

To implement fingerprint recognition technology in mobile displays, various approaches have been developed, including optical, ultrasonic, and capacitive methods [1-3]. Recently, the integration of organic photo diodes (OPDs) within OLED panels has been proposed as a promising solution. This approach enables high-resolution fingerprint recognition without separate sensor modules [4]. However, all of these methods still require additional sensing components within the display, which increases manufacturing costs and fabrication complexity.

To address these challenges, this paper proposes a novel micro-LED-based fingerprint recognition system that operates without any additional sensors within the display. This system operates on the principle that a reverse-biased micro-LED exhibits current flow, photocurrent, that varies depending on the intensity of the incident light. A readout circuit is implemented on a PCB using a charge integrator, enabling the detection of differences in photocurrent values between ridge and valley. Our proposed system adopts a differential sensing method to eliminate electronic noise, achieving high sensitivity that enables effective distinction between ridge and valley. Additionally, we propose to install black walls between LEDs to minimize direct light interference from emitting LEDs to sensing LEDs.

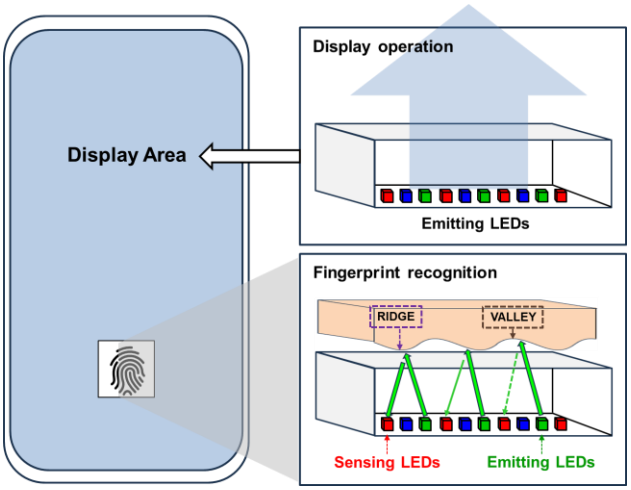

Figure 1. Proposed micro-LED display system featuring both display operation and fingerprint recognition.

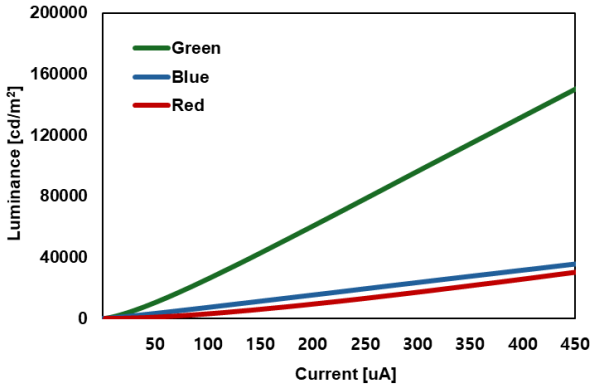

Figure 2. Luminance of micro-LEDs as a function of driving current.

2. Fundamental Characteristics of Micro-LEDs for Fingerprint Recognition

The micro-LEDs used in this study have a width and length of 125 μm and 200 μm, respectively, with a sub-pixel pitch of 200μm. Fig. 2 shows measured luminance values of RGB micro-LEDs as a function of driving current. The proposed system performs fingerprint recognition using photocurrent levels proportional to forward current of emitting LEDs. Therefore, to maximize the photocurrent through the sensing LED, we need to use maximum current of micro-LEDs in display operation.

Target luminance is set to 2,000 cd/m^2, because maximum luminance of commercially available smartphones is approximately 2,000 cd/m^2. The RGB luminance ratio required

ISSN 0097-996X/25/5601-0154-$1.00 © 2025

for full-white is set consistent with that of commercially available smartphones. Thus, to achieve a luminance of 2,000 cd/m^2, the required luminance for green and blue LED are determined to be 1,429 cd/m^2, and 155 cd/m^2, respectively [5]. Since light emitted from emitting LEDs must have higher energy than that of sensing LEDs, the emission current of red LEDs is not considered. Assuming an aperture ratio of 1% for the display, the luminance required from the green and blue LEDs is 142,900 cd/m^2 and 15,500 cd/m^2, respectively [6]. Accordingly, the required currents are 400 μA and 200 μA for green and blue LEDs, respectively.

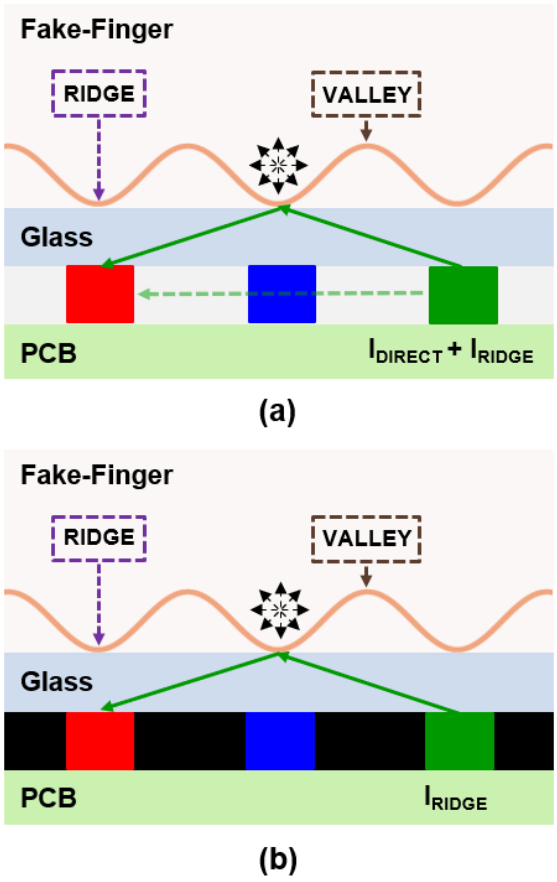

Figure 3. Conceptual cross-section views(a) without black wall fabrication (b) with black wall fabrication.

Fig. 3 shows conceptual cross-sectional views of a micro-LED pixel structure without and with black wall fabrication. In the proposed system, ridge and valley are distinguished by utilizing only the light reflected from the cover glass interface and the fake-finger surface. To achieve this, minimizing direct light interference from emitting LEDs to sensing LEDs is critical.

To address this issue, the space between LEDs is filled with a liquid material, which was subsequently cured to form a solid black wall structure. Fig. 3(a) illustrates that direct light from emitting LED reaches sensing LED, making it difficult to distinguish reflected lights from ridge and valley. In contrast, Fig. 3(b) illustrates that black wall absorbs the directly incident light, enabling the system to distinguish reflected lights from ridge and valley. This confirms that the black wall's effectiveness in mitigating direct light interference, thereby enhancing the system's sensitivity.

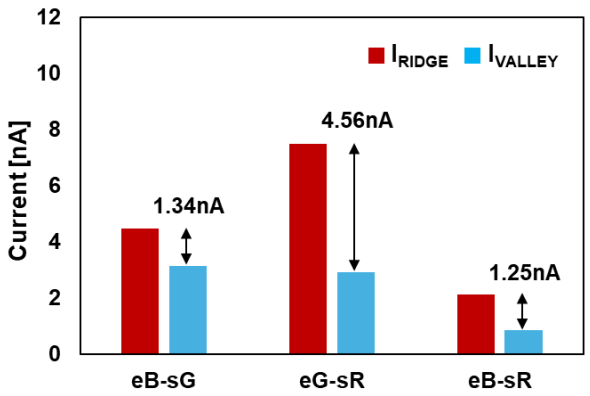

Figure 4. Comparison of photocurrent values under ridge and valley for each emitting-sensing LED combination.

Fig. 4 shows the photocurrent values and their differences between ridge and valley for various combinations of emitting and sensing LEDs. To compare photocurrent characteristics for each combination, our scaled-up experimental setup emulates an actual mobile display with 300 ppi and 70 μm-thick cover glass. A 500 μm-thick cover glass was placed over the LEDs, and a scaled-up fake-finger was positioned on top. The fake finger, made from a material with the same refractive index as human skin, was designed in white to mimic the scattering phenomena of a real finger [7].

To generate sufficient photocurrent for fingerprint recognition, the energy bandgap of the emitting LED must be larger than that of the sensing LED. Based on this principle, photocurrent characteristics were compared and analyzed for three specific combinations: eG-sR, eB-sR, and eB-sG. The driving currents for emitting LEDs were set to 400 μA for green and 200 μA for blue, as calculated earlier. The results showed that the difference in photocurrent values between ridge and valley was 4.56 nA for eG-sR, 1.25 nA for eB-sR, 1.34 nA for eB-sG. This shows that the eG-sR combination exhibits the highest sensitivity in distinguishing between ridge and valley, making it the optimal choice for fingerprint recognition.

3. Sensing Circuit and Measurement Results

Fig. 5(a) and 5(b) illustrate the proposed sensing circuit and timing diagram of signals, respectively. The operation of the proposed sensing circuit is divided into four stages: (1) $T_{PROGRAMMING}$ (T_{PG}), (2) $T_{INITIALIZATION}$ (T_{INI}), (3) T_{SENSE}, (4) T_{HOLD}. During T_{PG}, the Store signal goes high, storing the Sensor signal in C_{ST}. When the Sensor signal is high, the corresponding LED operates as a sensing LED, but when it is low, it functions as an emitting LED.

For display operations, a constant current flows through the LED, driven by the PDIC (pixel driving integrated circuit) which operates as a current-sinking IC. The operational principle and driving waveforms of the PDIC are detailed in our previous study [8]. For sensing operations, during T_{INI}, the Integration signal goes high, initializing the output of the charge integrator, V_{SENSE}, to Vref. Before T_{INI} ends, the Read signal is set to low, causing Vref to be applied to the cathode of the LED, which results in a reverse bias across it. In T_{SENSE}, the Integration signal goes high while the Read signal remains low. During this stage, the photocurrent generated by incident light is sensed through the charge integrator. As the intensity of incident light on the LED increases, photocurrent also increases, causing the V_{SENSE} to rise

steeply. In contrast, when the intensity of the incident light is lower, photocurrent decreases, causing the V_{SENSE} to rise gradually. If the Read signal remains low without transit to high, the photocurrent will cause the V_{SENSE} value to keep increasing until it saturates at the supply voltage of the charge integrator, 12 V. Therefore, to clearly distinguish between ridge and valley, it is crucial to set an appropriate sensing time by carefully considering factors such as the time required for fingerprint recognition and the specifications of the target display.

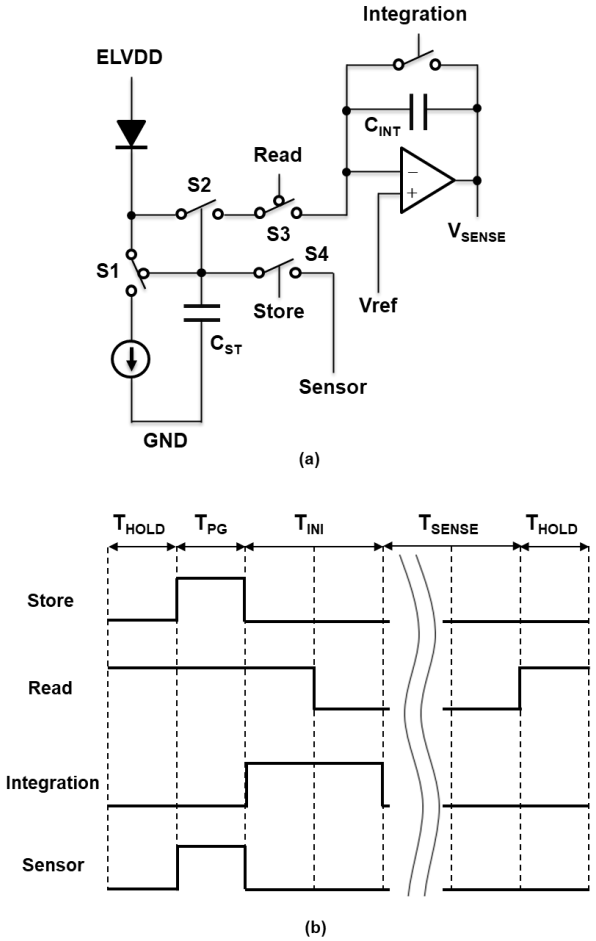

Figure 5. (a) Schematic of the sensing circuit utilizing a charge integrator (b) timing diagram of signals for the proposed circuit.

The target performance of the proposed system is to successfully recognize fingerprints within 1.5 s, regardless of the sensing area, on a display with a resolution of 352 × 430 and a refresh rate of 60 Hz. To achieve this, a single readout circuit must sequentially sense all pixels in the vertical direction within 1.5 s. In this case, the sensing operation is assumed to occur only during vertical blank time to avoid affecting the display operation. Given that the vertical blank time is 1.75 ms, there are 89 vertical blank times within 1.5 s, resulting in a total available sensing time of 155.75 ms. This means the charge integrator must sequentially sense photocurrents from 430 pixels within 155.75 ms. To sequentially sense 430 pixels within 155.75 ms, each pixel must be sensed within 360 μs. Based on these calculations, the proposed system assigns 10 μs for T_{INI}, 300 μs for T_{SENSE}, and 40 μs for T_{HOLD}.

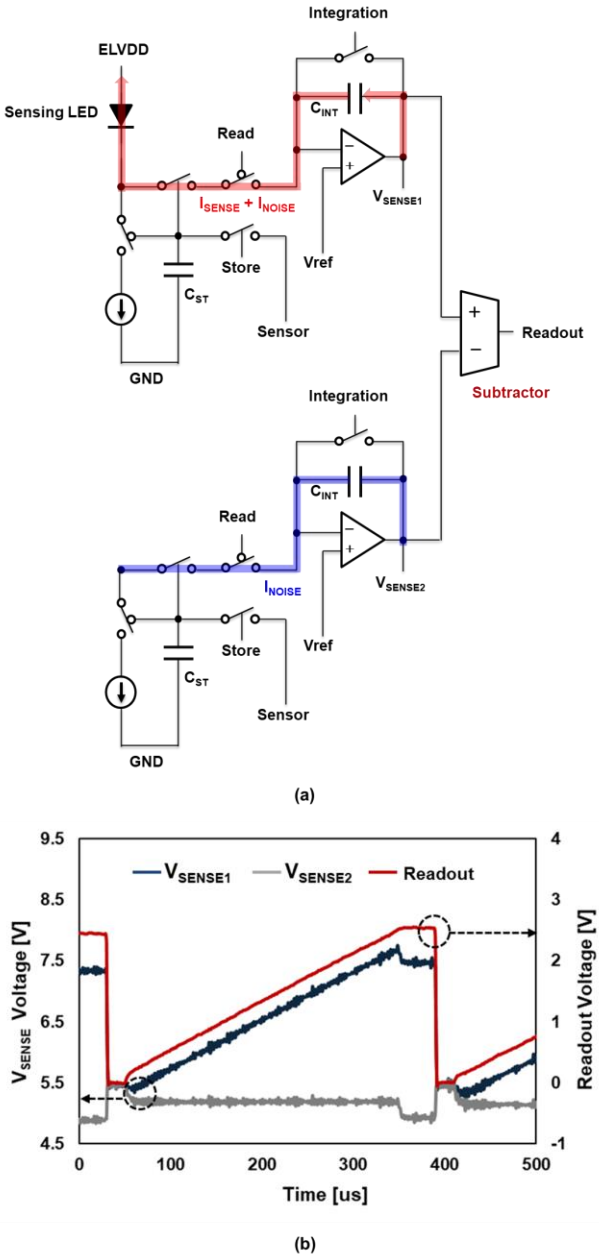

Figure 6. (a) Schematic of the differential sensing method (b) integration results of the charge integrator before and after applying the differential sensing method

Fig. 6(a) illustrates the schematic of the differential sensing method utilized in the proposed system, while Fig. 6(b) shows the integration results of the charge integrator before and after applying the differential sensing method. The charge integrator integrates all the current flowing through C_{INT}. As a result, it senses not only photocurrent generated by micro-LED but also noise currents produced in display panel. When the level of electronic noise increases, it may become difficult to distinguish between ridge and valley in real time.

To address this issue, the differential sensing method was applied, and its effectiveness was validated by using two adjacent sensing circuits. Both charge integrators operate with the same control signal, with one connected to the cathode of the sensing

LED, while the other has nothing connected to its input. As a result, the charge integrator connected to the sensing LED integrates both photocurrent I_{SENSE} from the LED and noise current I_{NOISE} from display panel. In contrast, the charge integrator without any input connection integrates only the noise current I_{NOISE}. By subtracting the integrated output of the second charge integrator from the first, the system isolates photocurrent I_{SENSE}. This differential output is then used as the final readout voltage, effectively eliminating electronic noise. As shown in Fig. 6(b), the degree of coupling in the output voltage caused by the switch control signals has been reduced, and the noise-induced ripples have been eliminated. This indicates that utilizing the differential sensing method enables the differentiation of ridge and valley with high-sensitivity.

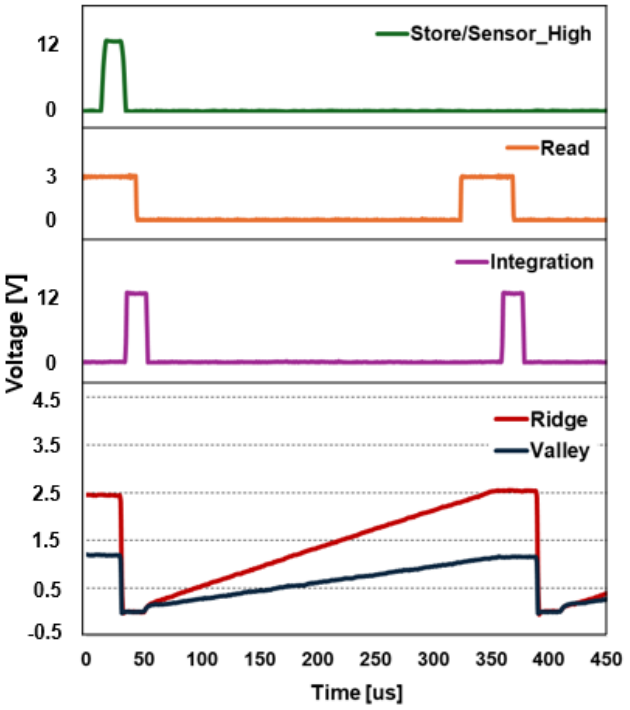

Figure 7. Measured waveforms of control signals for sensing and readout voltage

Fig. 7 shows the sensing results for the ridge and valley conditions of a fake-finger in the proposed fingerprint recognition system, using an eG-sR combination with an emission current of 400 μA and a light sensing time of 300 μs. By applying differential sensing method, the noises were eliminated, resulting in clean waveforms. The integration capacitor, C_{INT}, was designed with a value of 1 pF, resulting in a 1.38 V difference in the readout voltage for a photocurrent difference of 4.56 nA during the sensing time. This demonstrates the potential of the proposed system to achieve fingerprint recognition within 1.5 s in a 352 × 430 array environment without any additional sensors with high-sensitivity.

4. Conclusion

In this paper, we propose a novel fingerprint recognition system that utilizes reverse-biased micro-LEDs as photodetectors, enabling fingerprint recognition across the entire display without the need for additional sensors. We implemented readout circuits using charge integrators and validated the feasibility of the proposed system by successfully distinguishing between ridge and valley of a fake-finger. Additionally, we employed a differential sensing method to effectively eliminate electronic noise from the display panel, thereby achieving enhanced sensitivity. These results demonstrate the potential of the proposed system for high-sensitivity, sensor-free fingerprint recognition in mobile display environments.

5. Acknowledgements

This work was partially supported by the National Research Foundation of Korea (NRF) grant funded by the Korea government (MSIT) (No. RS-2023-00253537) and this work was supported by the BK21 Plus Program (Future oriented innovative brain raising type, 21A2013000 0018) funded by the Ministry of Education (MOE, Korea) and the National Research Foundation of Korea (NRF).

6. References

[1] T. Shimamura, H. Morimura, S. Shigematsu, M. Nakanishi, and K. Machida, “Capacitive-sensing circuit technique for image quality improvement on fingerprint sensor LSIs,” *IEEE Journal of Solid-State Circuits*, vol. 45, no. 5, pp. 1080–1087, 2010, doi:10.1109/JSSC.2010.2042525.

[2] B. S. W. Back, Y. G. Lee, S. S. Lee, and G. S. Son, “Moisture-insensitive optical fingerprint scanner based on polarization resolved in-finger scattered light,” *Optics Express*, vol. 24, no. 17, pp. 19195–19202, 2016, doi:10.1364/OE.24.019195.

[3] S. Memon, M. Sepasian, and W. Balachandran, “Review of fingerprint sensing technologies,” in *Proceedings of the 12th IEEE International Multitopic Conference*, 2008, pp. 226–231, doi:10.1109/INMIC.2008.4777740.

[4] T. Kamada, R. Hatsumi, K. Watanabe, S. Kawashima, M. Katayama, H. Adachi, T. Ishitani, K. Kusunoki, D. Kubota, and S. Yamazaki, “OLED display incorporating organic photodiodes for fingerprint imaging,” *Journal of the Society for Information Display*, vol. 27, no. 6, pp. 361–371, 2019, doi:10.1002/jsid.786.

[5] Y. J. Ko, D.-H. Jeon, W.-B. Jeong, M. G. Lim, and S.-W. Lee, “Bit depth of drivers for micro-LED displays adopting low-temperature polysilicon oxide thin-film transistors,” *IEEE Journal of the Electron Devices Society*, vol. 11, pp. 161–166, 2023, doi:10.1109/JEDS.2023.3250605.

[6] E. L. Hsiang, Z. Yang, Q. Yang, Y. F. Lan, and S. T. Wu, “Prospects and challenges of mini-LED, OLED, and micro-LED displays,” *Journal of the Society for Information Display*, vol. 29, no. 6, pp. 446–461, 2021, doi:10.1002/jsid.1058.

[7] D.-H. Jeon, W.-B. Jeong, H.-J. Chung, and S.-W. Lee, “Novel micro-LED display featuring fingerprint recognition without additional sensors,” *IEEE Access*, vol. 10, pp. 74187–74197, 2022, doi:10.1109/ACCESS.2022.3190608.

[8] Y. S. Joung, W. B. Jeong, M. J. Ko, J. I. Kim, H. S. Park, J. H. Kim, and S. W. Lee, “Implementing a photo-detectable AM-LED display using discrete ICs,” in *SID Symposium Digest of Technical Papers*, vol. 55, no. 1, pp. 841–844, 2024, doi:10.1002/sdtp.17718.